Global calibration of SARAL/AltiKa using multi-mission sea surface height crossovers

Denise Dettmering, Christian Schwatke & Wolfgang Bosch

Abstract

In March 2014 SARAL/AltiKa completed its first year in orbit. The 1 Hz GDR-T data of the first 10 cycles of the mission is used to perform a comprehensive quality assessment by means of a global multi-mission crossover analysis. Within this approach, SARAL sea surface heights are compared with data from other current missions, mainly Jason-2 and Cryosat-2, to reveal its accuracy and consistency with the other altimeter systems. Alongside with global mean range bias and instrumental drifts, investigations on geographically correlated errors as well as on the realization of the systems origin are performed. The study proves the high quality and reliability of SARAL. The mission shows only a small range bias of about - 5 cm with respect to Jason-2 and neither significant time-tag bias nor instrumental drifts. With 1.3 cm the scatter of radial errors is in the same order of magnitude as for Cryosat-2 and Jason-1 GM and will probably further improve using an enhanced sea state bias (SSB) model. However, the wet tropospheric corrections from SARAL radiometer still show some systematic effects influencing the range bias as well as geographically correlated error patterns and the z-component of the origin. Improved inflight calibration will be necessary to overcome these effects.

1. Introduction

The “Satellite with ARgos & Altika” (SARAL) is a French/Indian mission developed as collaboration between ISRO and CNES (CNES, 2013). SARAL was launched on February 25, 2013 and is equipped with two independent main payloads: ARGOS-3 and AltiKa. The latter is an innovating single-frequency altimeter system measuring in Ka-band (35.75 GHz) – the first one in orbit. In comparison to classical Ku/C-band altimeters (such as those on board of TOPEX, Jason, and ENVISAT), the AltiKa footprint is reduced and an improved along-track resolution is reached. Moreover, AltiKa works with an enhanced bandwidth of 500 MHz (CNES, 2013) and therefore yields an improved range resolution. The abdication of a second frequency is admissible as the main frequency is relatively high and allows neglecting most of the ionospheric effects (which are proportional to the inverse of the squared frequency). The remaining influence can be easily eliminated using an ionospheric model such as IGS GIM (Hernández-Pajares et al, 2009). However, since Ka-band measurements show an increased sensitivity to rain and clouds, reduced data availability is to be expected.

SARAL follows the same orbit with a sun-synchronous 35-day repeat cycle as the multi-disciplinary phases of ERS-1 (1991-2000), ERS-2 (1995-2011), and ENVISAT (2002-2012) missions extending the long time series from 1991 to 2010 (between 2010 and 2012 ENVISAT flew on a drifting orbit). In order to connect the SARAL time series to ENVISAT a careful validation and calibration of the new mission is necessary. Even more important is to ensure the consistency to other current altimeter missions such as Jason-2, Cryosat-2, and HY-2A allowing multi-mission altimetry applications. This will improve the spatial and temporal resolution for manifold applications regarding ocean dynamics and variability.

As ENVISAT had been already decommissioned when SARAL was launched, no tandem flight phase for cross-calibration and validation was possible as for TOPEX/Jason-1 (Beckley et al., 2004) and Jason-1/Jason-2 (Beckley et al., 2009). Consequently, other calibration methods are necessary. Certainly, one will use absolute calibration approaches on dedicated in-situ calibration sites as already done e.g. for ENVISAT in Corsica (Bonnefond et al, 2013) and for other missions in Harvest (Haines et al, 2010) and Bass Strait (Watson et al, 2011). For SARAL, a new calibration

site in the Indian ocean south of India has been established, called Kavaratti, and first results for bias estimates were presented by (Babu, 2014).
Global calibration approaches based on crossover analysis are complementary to these absolute calibrations at individual sites. Cross-calibration provides only relative information with respect to other missions, but on a global scale. Classically, a cross-calibration is performed using two different missions (e.g. Prandi et al, 2014). In this study, a multi-mission crossover analysis (MMXO) is used to estimate radial errors for all contemporaneous missions involved in the procedure. The main goal is to combine all systems and to perform multi-mission altimetry (Bosch et al., 2014). On the other hand, the interpretation of the estimated radial errors reveals problems within the measurements data, e.g. instrument drifts, orbit errors, uncertainties in the used correction models or measurements (such as radiometer correction or sea state bias (SSB)). This was already demonstrated for Jason-2 (Dettmering and Bosch, 2010a) and ENVISAT (Dettmering and Bosch, 2010b).
First selected results for the SARAL mission were recently provided in Bosch et al. (2014), based on about 4.5 months (4 cycles) of SARAL patch 1 data. In the paper on hand, results for the first year of SARAL data are presented based on 10 cycles of 1Hz GDR-T data, patch 2 (CLS 2014a). The focus of this paper is not to provide an exhaustive quality assessment of the SARAL mission data but to check one basic product, the SARAL-derived sea surface heights (SSH). The paper is separated in 5 sections: Section 2 introduces the method used for the calibration. Afterwards, the used data sets are presented (Sect. 3). Section 4 compiles the results before the paper finishes with a concluding chapter.

2. Fundamentals of the Multi-Mission Crossover Analysis

By using redundant measurements of the sea surface a multi-mission crossover analysis (MMXO) aims to estimate relative radial errors for all altimeter systems operating simultaneously. Thus, a consistent and simultaneous calibration of more than one mission can be performed. This is one basic distinction to classical two-mission cross-calibration methods. The present approach, described in detail in (Bosch et al, 2014), does not use an analytic function (such as piecewise polynomials or splines) for modeling the radial errors but rely on a discrete modeling to estimate the radial errors in a least squares adjustment. For this purpose, SSH crossover differences (single-satellite and dual-satellite) as well as the differences of consecutive measurements of the same mission are minimized in an adjustment process using weighting functions and variance component estimation. The minimization of consecutive differences ensures a certain smoothness of the time series of radial errors without implying restrictive assumptions about the error characteristics.
All computations are done with respect to one reference mission in order to overcome a rank defect of the system to be solved. As a consequence, only relative calibrations are performed, in this study with respect to Jason-2.
In order to deal with the large amount of data – for the whole study about 650 000 crossover differences are used which leads to a total number of unknowns of approximately 1.2 million – all computation are performed in smaller time segments of 10 days, corresponding to the cycles of the references mission (Jason-2) and yielding between 10 000 and 35 000 crossovers per segment.
The main outputs of MMXO are time series of radial errors for every mission involved in the analysis. These time series might be used for correcting the original data sets in order to provide a homogeneous long-term data set with optimal spatial and temporal resolution.
In addition, the time series of radial errors can be used to obtain further information describing the quality and consistency of each mission. In detail these are:

- Stochastic properties, especially empirical auto-covariance functions
- Geographically correlated mean errors
- Range biases (global mission means and with ten days resolution)
- Information on center-of-origin realization and low-order harmonics

More details on the theory of MMXO and the resultant quantities are provided in Bosch et al., 2014.

3. Data used for investigations

SARAL was launched on February 25, 2013 and the first AltiKa data were disseminated mid of March, 2013. At the time of writing, 10 cycles (each with a period of 35 days) of SARAL GDR data are available covering a time period of nearly one year. Within this period data from the following additional missions are available: Jason-1 (up to June 2013; on its geodetic orbit), Jason-2, Cryosat-2, and HY-2A. As the data from HY-2A seems not reliable in its present state (cf. Bosch et al., 2014) this mission is discarded for the present study.

The SARAL data used in this investigation is based on the GDR-T data set, patch 2 (CLS, 2014a) available from AVISO at ftp://avisoftp.cnes.fr/AVISO/pub. GDR-T is a temporary product but uses the same processing standards as GDR-D products. In order to ensure maximum consistency to the other missions within the study some of the included corrections are replaced by external information as listed in Table 1. For all missions, the orbit as well as the ionospheric dual-frequency correction and the wet tropospheric correction (from microwave radiometer, MWR) remain unchanged for most of the analyses performed since both are assumed to provide the best possible quality. However, some dedicated investigations are performed in order to quantify the influence of the radiometer correction on the SARAL products.

Table 1: data set used within this study

	SARAL	**Jason-2**	**Jason-1 GM**	**Cryosat-2**
cycle	**1…10**	**173…207**	**528…537**	**38…51**
altimeter range	GDR-T	GDR-D	GDR-C	GDR, Baseline B
orbit	GDR-T	GDR-D	GDR-D	GDR, Baseline B
	(all missions are based on ITRF-2008)			
Earth tides	GDR-T	GDR-D	GDR-C	GDR, Baseline B
	(all missions use Cartwright and Edden, 1973)			
ocean tides	EOT11a (Savcenko and Bosch, 2012)			
atmospheric correction	Dynamic Atmospheric Correction (DAC)[1]			
SSB	GDR-T	GDR-D	GDR-C	GDR, Baseline B
ionosphere	GDR-T, GIM model (JPL)	Smoothed Dual-frequency	Smoothed Dual-frequency	GDR, GIM model
dry troposphere	GDR-T	GDR-D	GDR-C	GDR, Baseline B
	(all from ECMWF atmospheric pressures and model for S1 and S2 atmospheric tides)			
wet troposphere (main)	MWR	AMR enhanced product (Brown, 2010)	JMR enhanced product (Brown, 2010)	model (ECMWF)
wet troposphere (tests)	GDR-T	GDR-D	GDR-C	GDR, Baseline B
	(all from ECMWF model)			

SARAL is equipped with a dual-frequency microwave radiometer (MWR) for deriving the wet troposphere range correction. This is computed using the measured brightness temperatures together with a neural network approach (CNES, 2013). Since the SARAL radiometer measures on two frequencies only (in contrast to Jason-2 with three frequencies), the altimeter estimated backscatter

[1] DAC are produced by CLS Space Oceanography Division using the Mog2D model from Legos and distributed by Aviso, with support from Cnes (http://www.aviso.oceanobs.com/).

coefficient has to be used to account for the surface roughness in order to replace the third (low-frequency) channel. This is the same approach as applied for ENVISAT (Obligis et al., 2006) and ERS-2 (here the altimeter wind speed is used instead of the backscatter coefficient).
The atmospheric models provided within the SARAL GDR-T data set are identical to the models used by Jason-2.
The SSB model currently provided within SARAL GDR-T data set is a preliminary product, derived from a hybrid look-up table but actually based exclusively on the significant wave height (CLS, 2014a). This will probably degrade the quality of the current SARAL data set.
For the global multi-mission crossover analysis all open-ocean SSH crossover differences with time difference below two days are used. Coastal areas as well as crossover points with SSH differences larger 1 m or standard deviations exceeding 0.1 m are discarded.

4. Results

The MMXO reduces the residuals of crossover differences from about 0.10 - 0.16 m to values around 4 cm (standard deviations). This corresponds to an improvement of 72% to 95% percent, depending on the missions available in each segment.
The relative weighting between different satellite missions is done automatically by means of variance component estimation (VCE, for detailed information including formulae refer to Bosch et al, 2014). For each 10 day segment, variance components (VC) are estimated for each mission. However, they cannot be used to provide absolute information on the quality of the single missions but reveals details on the relative mission behavior. The smaller the VC, the higher is the weight of a mission. As the references mission (i.e. Jason-2) is forced to a constant mean value per cycle, its VC normally is smaller and smoother than the other missions. Table 2 summarizes the mean VC for the missions showing the smallest values for Jason-2. The weight of SARAL is located between Jason-1 and Cryosat-2. Using model corrections for the wet troposphere instead of radiometer measurements slightly improves the VC for SARAL (from 0.1411 to 0.1289, about 9%). The estimated VC will strongly impact the scatter of radial errors discussed in the following section. The temporal variation of VC is moderate for all missions reflecting short-time effects due to orbit maneuvers, geophysical effects or measurement uncertainties.

Table 2: Estimated variance components (average of all cycles) using two types of wet tropospheric correction (no unit)

	Jason-2 (reference)	SARAL	Cryosat-2	Jason-1 GM
MWR	0.0618	0.1411	0.1539	0.1063
model	0.0619	0.1289	0.1463	0.1067

4.1 Radial errors and its stochastic properties

The main output of MMXO is one time series of relative radial errors for each mission included in the analysis (cf. Sect. 2). For the reference mission Jason-2 radial errors are estimated, too. The absolute level of Jason-2 radial errors is the only quantity fixed: for each cycle to -0.005 m. This value has been computed from the overlapping times with Jason-1 and TOPEX and it ensures that all radial errors are given with respect to TOPEX (Bosch et al., 2014). As the radial error estimates are based on SSH differences, they represent the overall accuracy of the missions as they do include orbit errors, as well as altimeter range errors, and uncertainties of geophysical corrections. The only way to separate the different influences is to re-compute the SSH with other parameters and compare both MMXO solutions with each other.
In order to judge the quality of radial errors some stochastic properties of the time series are

analyzed: average and standard deviation, auto-covariance function, and power spectra. The mean value of the radial errors (given in Table 3) is strongly correlated to the mean range bias handled in more detail in section 4.3. The standard deviation describing the temporal (and spatial) variability of the radial errors yields 1.3 cm for SARAL (cf. Table 3). This is larger than for Jason-2, however, it is in the same order of magnitude than Jason-1 GM and Cryosat-2. That might be partly related to the fact that Jason-2 serves as reference mission. Moreover, since the accuracies of geophysical corrections have a huge impact to the scatter of radial errors, another important contribution is due to SSB model corrections. Keeping in mind that the SSB model for SARAL is still a primary one and will probably improve in the future, this is a very promising result for SARAL which is expected to further improve in the future. It is important to note, that the values in Tab. 3 are not directly comparable to results from classical crossover analysis. In order to extract complete error information the standard deviations of the residual crossover differences have to be taken into account, too, which are around 4 cm (see beginning of Sect. 4).

Table 3: Mean and standard deviation of radial errors [cm]

	Jason-2 (reference)	SARAL	Cryosat-2	Jason-1 GM
MWR	-0.49 +- 1.04	-5.10 +- 1.34	-24.63 +- 1.32	10.62 +- 1.36
model	-0.49 +- 1.05	-5.22 +- 1.29	-25.28 +- 1.28	10.58 +- 1.34
# xover	~390 000	~ 330 000	~165 000	~110 000

Table 3 also shows the number of (valid) crossover differences available for each of the missions. As expected (due to data outages because of rain) SARAL produces less crossovers than Jason-2. The difference yields about 60000 values, approximately 15%. This is in the same order of magnitude as former comparisons revealed for ENVISAT. However, SARAL has still twice as many valid crossovers than Cryosat-2. Jason-1 should not be used as comparison since its results are not based on the full year of investigation.
Using model information for wet troposphere corrections instead of radiometer measurements, the behavior of Jason-1/2 remains unchanged whereas the values for SARAL and Cryosat-2 slightly decrease. This indicates that the MWR-derived corrections of SARAL patch2 are less reliable than the model-derived corrections. This is in accordance to Picard et al (2014) who showed that the performance of SARAL radiometer is similar to Jason-2 around the Equator (±20°) but currently still degraded in polar regions (mainly below 40° south) due to some remaining problems in the neural network algorithm. As Cryosat-2 is not equipped with a radiometer, one assumes its radial errors to stay constant which is not true. The effects from other missions leak in here. The standard deviations of the radial errors are strongly correlated with the result of VCE (see Table 2).

The standard deviation of radial errors comprises not only random errors but also systematic effects which can be identified by further investigations. In order to check the time series for systematic parts a frequency analysis is performed and a power spectrum for each mission is computed. Figure 1 shows the results for SARAL (using the radiometer wet troposphere correction). One can clearly identify periods of about 0.07 days in the radial errors of SARAL – and also in the other missions (not shown). These effects represent the orbital period and they are caused by precise orbit determination (POD) (1/rev effect). For SARAL the amplitude yields 2.7 mm in comparison to 1.5 mm for Jason-2, and 2.4 mm for Cryosat-2. This indicates that for Jason-2 the POD is slightly more accurate than for Saral, especially concerning systematic components in the 1/rev empiricals. Improvements are expected soon, as after a complete beta prime cycle (~1 year) a calibration of this parameter is possible (Cerri et al, 2013, Couhert et al, 2014). For Jason-1 no analysis is performed since the time series only comprises very few cycles.
Using ECMWF model corrections for the wet troposphere cause the half-daily signals in the radial errors to become more prominent for all missions. For Cryosat-2 it is the most prominent period

with amplitude of 3.4 mm.

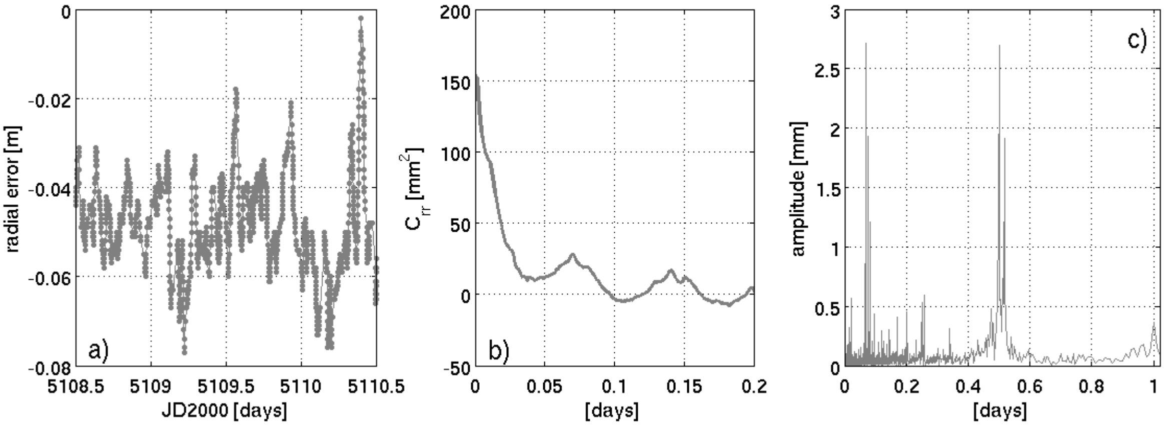

Figure 1: Radial errors of SARAL (plot a), 2-day subset for Dec 2013, 27-29), derived empirical auto-covariance function C_{rr} (plot b), from whole time series), and related power spectrum (plot c)) based on data corrected by radiometer wet troposphere.

Analyzing the radial errors separately for ascending and descending errors shows no evidence for significant time tag bias in the data as reported for example for Cryosat (Dettmering and Bosch, 2014).

4.2 Geographically correlated mean errors

The radial errors are used to estimate geographically correlated mean errors (GCE). These are errors having the same sign for ascending and descending satellite passes. They cancel out in single-satellite crossover differences. However, due to their systematic nature they directly map in sea surface height estimates. GCE are computed by gridding the ascending and descending radial errors separately after subtracting a cycle-average and building the mean values for each grid cell (2.5° by 2.5°) following the theory of (Rosborough, 1986). In comparison to other ("classical") computation methods, the GCE from MMXO comprise not only orbit errors from POD but also systematic effects coming from geophysical corrections and instrumental influences. However, as the result is not based on standard crossover differences of two missions, the noise level is reduced.

Two different solutions are computed based on different wet troposphere corrections. All GCE remain smaller than 1 cm (with only few outliers) and yield averages of -0.03 ± 3.14 mm using the model correction and -0.19 ± 3.56 mm using the radiometer correction. The geographical distribution is illustrated in Figure 2. Although the errors are small, one can see some systematic effects, especially in the right plot which is based on the radiometer correction.

This becomes even clearer analyzing the temporal behavior of the GCE instead of the complete time series of radial errors as a whole. For this purpose, the time series of SARAL radial errors has been separated into four segments comprising about 100 days each (10 Jason-2 cycles). The resulting GCE patterns differ considerably. For the time period of cycle 180-189 (May to August 2013) GCE up to 2 cm occurred with a clear geographic pattern (not shown). As a reliable computation of GCE for shorter time periods is not possible, a detailed investigation on temporal effects will not be performed here. Time-dependent effects will be discussed in more detail based on center-of-origin parameters (c.f. Sect. 4.4.).

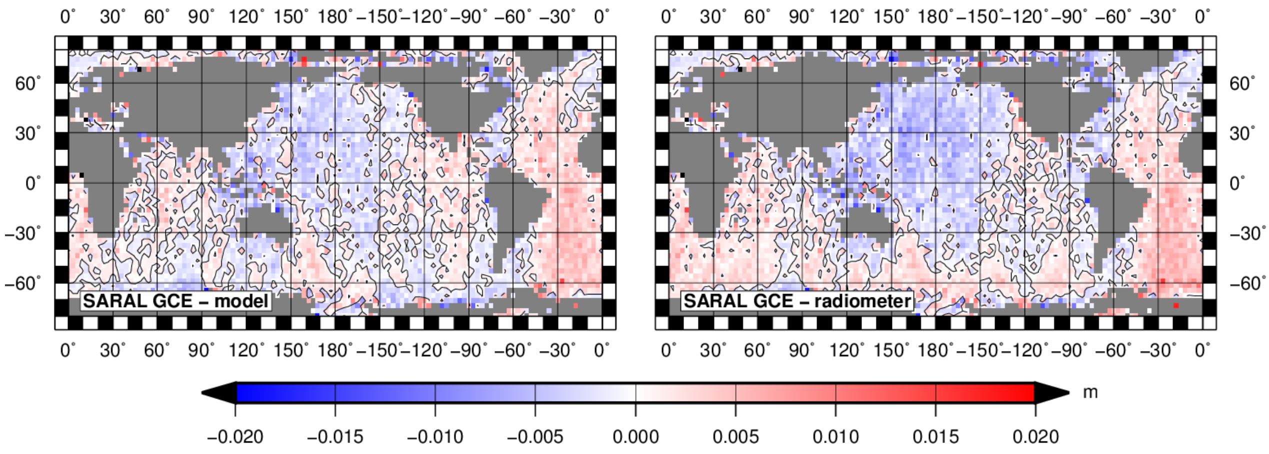

Figure 2: Geographically correlated mean errors for SARAL (left-hand side: based on model troposphere corrections; right-hand side: based on radiometer data (mixed solution))

4.3 Range bias

An important quantity from each altimeter calibration is a range bias caused e.g. by instrumental delays. In order to separate this range bias from other effects which are induced for example from POD a fragmentation of the radial errors is performed. For this purpose, the radial errors are approximated by a spherical harmonic series up to a degree of 2 (Bosch et al, 2014). The harmonic coefficient C_{00} equals the mean range bias. This post-processing step can be applied to the full time series of radial errors or to subsets. In the latter case, one can monitor the temporal variation of the parameters and conclude on possible drifts or other time-variable systematic effects.

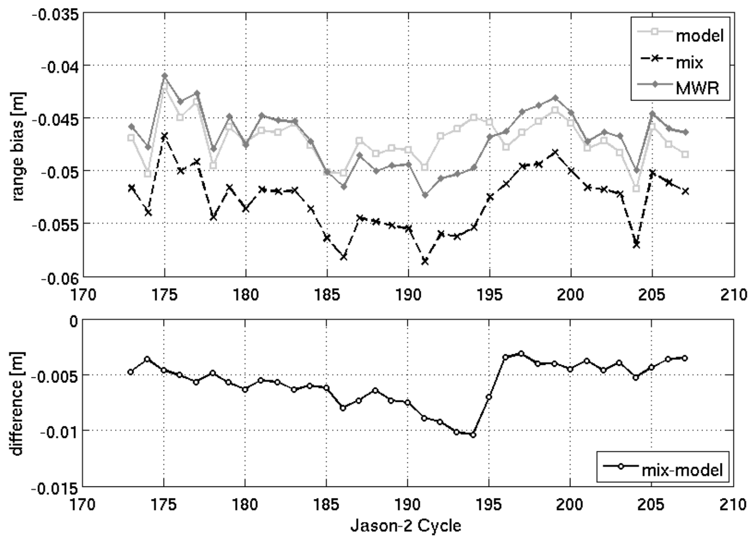

Figure 3: SARAL relative range bias with respect to Jason-2 (top plot) based on different wet tropospheric corrections (blue diamonds: radiometer; orange squares: model; dotted green: only SARAL radiometer) and influence of SARAL radiometer on relative range bias (bottom plot)

Figure 3 illustrates the relative range bias of SARAL with respect to Jason-2 with a temporal resolution of 10 days (Jason-2 cycles). The top plot shows in dark grey (diamonds) the result based on radiometer wet tropospheric corrections for SARAL and for Jason-2 and in light grey (squares) the model-based range bias. Both time series yield a global mean range bias of SARAL of -0.047 m with respect to Jason-2 corresponding to a value of -0.052 m with respect to TOPEX. In order to investigate the influence of the SARAL radiometer on the range bias a third time series was computed which is plotted in black (dotted line, crosses). For its computation the radiometer correction was only applied to SARAL, all other missions are corrected by models. Due to a clear offset between model and radiometers this (mixed) time series gives an average range bias which significantly differs from the other two.

The bottom plot of Figure 3 shows the influence of the SARAL radiometer on the relative range bias (differences mixed-model). One can identify a clear drift in the first part of the time series and a step of about 6 mm within cycle 195. The mean difference is -5.7 mm. This behavior perfectly corresponds to the daily monitoring of wet troposphere differences given in (CLS, 2014b) and is due to the saturation of hot calibration counts influencing the 37 GHz brightness temperature of the radiometer. This problem of onboard parameterization was solved on October 22, 2013 (CLS, 2014b). The remaining mean offset of about -4.5 mm is probably due to the ECMWF model, as the same offset is detectable for Jason-2.

In this first year of SARAL data, a temporal drift of the relative range bias is not detectable, neither using the radiometer correction nor applying model values.

4.4 Center-of-Origin

By estimating spherical harmonic coefficients from the radial errors of each mission included in the MMXO, one can extract valuable information on systematic effects in the realization of the origin (mainly due to POD). Following (Bosch et al., 2014) seven low-order coefficients are estimated. The first harmonic coefficient C_{00} equals the mean range bias and is already discussed in detail in section 4.3. The degree-one coefficients (C_{10}, C_{11}, S_{11}) represent the center-of-origin shifts, the coefficient C_{20} indicates an error pattern affecting the flattening of the Earth figure, and C_{21} and S_{21} are related to the orientation of the Earth rotation axis.

In this section, the differences between the coefficients from SARAL and Jason-2 are analyzed to identify possible systematic differences between these two missions. As all models used for the computation of SSH are identical, no differences are expected. However, as the numbers given in Table 4 show, for some of the coefficients – mainly C_{10} and C_{11}- differences larger 1 mm between SARAL and Jason-2 occurs in the main solution using the radiometer wet troposphere correction. For most of the coefficients there is no significant influence from the used wet troposphere corrections. Only for the z-component of the origin (C_{10}) and the Earth flattening (C_{20}) one can see some differences.

Table 4: SARAL spherical harmonic coefficients estimated from radial errors, relative values with respect to Jason-2, mean values for about one year time period (35 Jason-2 cycles), in [mm]

	MWR	model	mix
$\Delta C_{10} \equiv \Delta z$	-1.31 ± 2.27	-0.38 ± 1.32	-1.45 ± 2.57
$\Delta C_{11} \equiv \Delta x$	1.68 ± 1.42	1.40 ± 1.42	1.98 ± 1.59
$\Delta S_{11} \equiv \Delta y$	-0.75 ± 1.78	-0.80 ± 1.81	-0.63 ± 1.86
ΔC_{20}	0.68 ± 0.67	-0.56 ± 0.71	0.20 ± 0.68
ΔC_{21}	-0.02 ± 0.90	-0.07 ± 0.88	0.04 ± 0.93
ΔS_{21}	-0.03 ± 1.02	0.09 ± 0.95	0.00 ± 1.07

Currently, none of the values given in Table 4 differ significantly from zero. However, looking at the temporal variability of single coefficients some systematic behavior is visible. Whereas for C_{11}

not temporal systematics can be detected, C_{10} show a clear minimum for summer 2013 (cycle178-188) and maxima for March 2013 and 2014 as visible from Figure 4. The effects on C_{20} are much smaller and probably are caused by correlations between the two coefficients. Figure 4 shows the differences in C_{10} between SARAL and Jason-2 with a temporal resolution of 10 days. Despite the short time period of only one year, one can identify an annual signal in the z-component of the origin which can be significantly reduced (but not eliminated) applying model corrections instead of radiometer corrections.

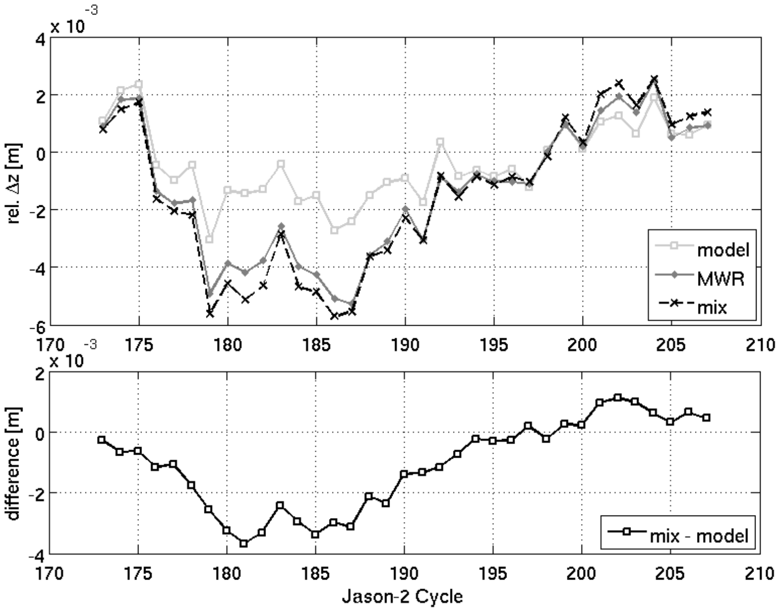

Figure 4: Differences in z-component of the origin between SARAL and Jason-2 using different wet troposphere corrections (top plot) and the influence of using radiometer instead of model corrections for SARAL (bottom plot).

In order to definitely assign the source of this effect to the radiometer, the wet troposphere correction differences itself were used to estimate origin-offsets. This was performed for SARAL, as well as for Jason-2 and for ENVISAT and is illustrated in Figure 5. In order to exclude effects from different sea ice extends and to make the results of missions with different inclinations comparable, only data for latitudes up to 50° (south and north) are used. One can clearly see that for all three missions annual signals are visible showing consistent periods (with maxima in July) but different amplitudes. For SARAL the effect is most prominent. As the model corrections should not depend on different orbits or satellites and moreover the orbits for Envisat and SARAL are identical, the source for this oscillation probably lays in the radiometer correction. Further investigations are necessary in order to fully understand this behavior. It might be related to the latitude-dependency of the quality of the neural network approach as reported by Picard et al. (2014).

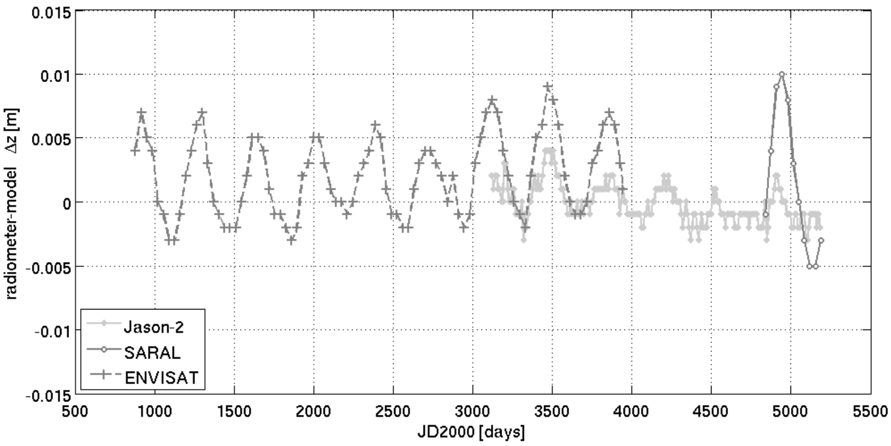

Figure 5: Differences between wet troposphere correction from radiometer and model (z-component of the origin) for a time period of twelve years (May 2002 to April 2014) for three different altimeter missions. Observations from high latitudes (latitude larger than 50°) are excluded.

The differences of the wet troposphere corrections (z-component) for all missions are in phase with the backscatter coefficient and the wind speed. The wet corrections themselves are slightly shifted. This indicates uncertainties in the consideration of the surface roughness. This assumption is strengthened by the fact, that the Jason-2 radiometer (AMR) showing the smallest z-component oscillations is equipped with a third frequency and does not rely on the altimeter estimated backscatter coefficient such as ENVISAT and SARAL. Moreover, the inflight calibration of the radiometer which is necessary to connect the measured brightness temperatures to the wet tropospheric delay is not yet as optimal for SARAL as for Jason-2 and ENVISAT (Picard et al, 2014).

5. Conclusion

The first year of SARAL GDR-T data yields high-accurate and reliable SSH values showing good consistency to existing missions such as Jason-2 and Cryosat-2. The global multi-mission crossover analysis reveals neither a significant time tag bias nor any instrumental drifts. The range bias shows no systematics and yields -4.7 ± 0.2 cm with respect to Jason-2 and -5.2 ± 0.2 cm with respect to TOPEX using model corrections for the wet troposphere.
However, further work is necessary to improve the radiometer-derived wet troposphere corrections. The current version evokes systematic effects in the range and in geographically correlated errors as well as in the realization of the origin. Mainly, in the z-component significant annual oscillations with amplitudes of about half a centimeter are visible.
As the work on the mission performance is still in process, improved data patches may be expected for the future. This will mainly comprises an enhanced SSB model and an improved inflight radiometer calibration and will surely improve the SARAL SSH.
But even today, the mission’s SSH data are of extreme value for various applications in altimetry as SARAL extends the long time-series of ESA satellite missions and complements Jason-2 and Cryosat-2 to provide high-resolution sea level products.

Acknowledgments

We would like to thank CNES/ISRO and AVISO for SARAL mission maintenance and data dissemination. Moreover, we gratefully acknowledge ESA and AVISO for providing the other mission data used for cross-calibration and the DAC corrections.

References

Babu, K.N. 2014. Absolute calibration of SARAL-AltiKa in Kavaratti during its initial Calibration-Validation phase. Presented at SARAL International Science and Applications Meeting 22-24 April, 2014, SAC Ahmedabad, available online at http://www.aviso.altimetry.fr/fileadmin/documents/ScienceTeams/Saral2014/22-04-2014/Session-3/KNBabuAltiKaApril2014.pdf (accessed on 2014-05-16)

Beckley, B., N. P. Zelensky, S. Holmes, F.G. Lemoine, R.D. Ray, S.D. Desai, S.T. Brown, and G.T. Mitchum, 2009. Assessment of Jason1 and OSTM Global Verification phase Sea Surface Height Collinear Residuals. Presented at OSTST Meeting 2009, Seattle, USA, available online: http://www.aviso.oceanobs.com/fileadmin/documents/OSTST/2009/oral/Beckley.pdf

Beckley, B., N. P. Zelensky, S. B. Luthcke, and P. Callahan, 2004. Towards a Seamless Transition from TOPEX/Poseidon to Jason-1. Mar. Geod. 37 (3), doi: 10.1080/01490410490889148

Bonnefond, P., P. Exertier, O. Laurain, T. Guinle, P. Femenias, 2013. Corsica: A Multi-Mission Absolute Calibration Site. In: Proceedings of 20 Years of Progress in Radar Altimetry Symposium, Venice, Italy, 24–29 September 2012; ESA SP-710

Bosch, W., D. Dettmering, and C. Schwatke, 2014. Multi-Mission Cross-Calibration of Satellite Altimeters: Constructing a Long-Term Data Record for Global and Regional Sea Level Change Studies. Remote Sensing, 6(3):2255-2281, doi:10.3390/rs6032255

Brown, S. A novel near-land radiometer wet path-delay retrieval algorithm: Application to the Jason-2/OSTM advanced microwave radiometer. IEEE Trans. Geosci. Remote Sens. 2010, 48, 1986–1992.

Cartwright, D. E. and Tayler, R. J., 1971, New computations of the tide-generating potential. Geophys. J. Roy. astr. Soc., 23(1), pp. 45-74

Cerri L., Couhert A., Houry S., Mercier F., Jalabert E. 2013. SARAL Precision Orbit Determination (MOE , POE). Presented at the 1st Saral/Altika verification workshop, Toulouse, France from 27 to 29 August 2013.

CLS, 2014a. Saral/Altika reprocessing GDR-T Patch2. CLS.DOS/NT/14-031, SALP-RP-MA-EA-22345-CLS, May 2013

CLS, 2014b. Saral GDR Quality Assessment Report, Cycle 009. SALP-RP-P2-EA-22250-CLS009

CNES, 2013. SARAL/AltiKa Products Handbook. Issue 2 rev 3, SALP-MU-M-OP-15984-CN, available online: http://www.aviso.oceanobs.com/fileadmin/documents/data/tools/SARAL_Altika_products_handbook.pdf

Couhert A., Houry S., Mercier F., Jalabert E., Moyard J. 2014. SARAL POD Status. Presented at the SARAL International Science and Applications Meeting, Ahmedabad, India, April 22, 2014

Dettmering D., Bosch , W. : Performance of ESA CryoSat-2 GDR data over open ocean. In: Ouwehand L. (Ed.) Proceedings of "CryoSat Third User Workshop", March 2013, Dresden, Germany, ESA SP-717 (CD-ROM), ISBN 978-92-9221-281-0, ESA/ESTEC, 2014

Dettmering D. and W. Bosch, 2010a. Global Calibration of Jason-2 by Multi-Mission Crossover Analysis. Marine Geodesy, 33:S1:150-161, doi:10.1080/01490419.2010.487779

Dettmering D. and W. Bosch, 2010b. Envisat radar altimeter calibration by multi-mission crossover analysis. Proceedings of the ESA Living Planet Symposium, Bergen, Norway, ESA Publication SP-686 (CD-Rom)

Hernández-Pajares M, Juan JM, Sanz J, Orus R, Garcia-Rigo A, Feltens J, Komjathy A, Schaer SC, Krankowski A, 2009. The IGS VTEC maps: a reliable source of ionospheric information since 1998. Journal of Geodesy, 83(3-4):263-275, doi:10.1007/s00190-008-0266-1

Haines, B.J., S.D. Desai and G.H. Born, 2010. The Harvest Experiment: Calibration of the Climate Data Record from TOPEX/Poseidon, Jason-1 and the Ocean Surface Topography Mission. Mar. Geod., 33:91–113, doi: 10.1080/01490419.2010.491028

Obligis, E., Eymard, E., Tran, N., Labroue, S., Femenias, P., 2006. First Three Years of the Microwave Radiometer aboard Envisat: In-Flight Calibration, Processing, and Validation of the Geophyhsical Products. Journal of Atmospheric and Oceanic Technology 23(6): 802-814, DOI: 10.1175/JTECH1878.1

Picard B., Frery M.-L., Obligis E. 2014. SARAL/AltiKa MWR Wet tropospheric correction Performances and Retrieval Strategies. Presented at the SARAL International Science and Applications Meeting, Ahmedabad, India, 22 to 24 April 2014.

Prandi P., Philipps S., Pignot V., Picot N., Guillot A. 2014. SARAL/AltiKa data quality assessment over ocean. Presented at the SARAL International Science and Applications Meeting, Ahmedabad, India, 22 to 24 April 2014.

Rosborough, G.W., 1986. Satellite Orbit Pertubations due to the Geopotential; Report CSR-86-1; Centre for Space Research, University of Texas: Austin, TX, USA

Savcenko, R.; Bosch, W. EOT11a - Empirical Ocean Tide Model From Multi-Mission Satellite Altimetry; Report 89; Deutsches Geodätisches Forschungsinstitut, München, Germany, 2012.

Watson, C., N. White, J. Church, R. Burgette, P. Tregoning, and R. Coleman, 2011. Absolute Calibration in Bass Strait, Australia: TOPEX, Jason-1 and OSTM/Jason-2. Mar. Geod. 31(3-4): 242-260, doi: 10.1080/01490419.2011.584834